Available online at www.sciencedirect.com
SCIENCE DIRECT®
Journal of Geodynamics 38 (2004) 161–184
JOURNAL OF GEODYNAMICS
http://www.elsevier.com/locate/jog

The present day rheology, stress field and deformation along the DSS profile FENNIA in the central Fennoscandian Shield

K. Moisio*, P. Kaikkonen

Department of Geophysics, University of Oulu, P.O. Box 3000, FIN-90014 Oulu, Finland

Received 9 September 2003; received in revised form 13 May 2004; accepted 24 June 2004

Abstract

The calculation of the rheological structure in the deep seismic profile FENNIA in the central Fennoscandian Shield allows in addition the modelling of the present-day stress field and state of deformation. Seismic and surface heat flow data together with all other applicable information are used in the construction of the model. Derivation of the two-dimensional rheological structure requires the determination of the temperature field and the use of known rheological laws both for the brittle and the ductile mechanisms. The rheological model is furthermore subjected to compressional loading resulting in the structural model, which is solved as well as the thermal model by the finite-element method. Results show that rheologically weak crustal layers can be generated under suitable conditions in the central Fennoscandian Shield. These are more evident when assuming wet conditions for the upper and middle crust. Although these weak layers are found the application of the rheological structure to a model, where stress and deformation are derived does not generate intensive crustal deformation. In the stress field influence of the rheology is very small in the crustal part whereas in the mantle a clear effect is seen at the depth of 100 km where plastic deformation begins. Uncertainties related to thermal modelling and how these affect rheological and structural modelling are also analysed in a quantitative form showing the importance of temperature in tectonic modelling.

1. Introduction

The deep seismic sounding (DSS) profile FENNIA is located in southern Finland and it runs from south to north in the Proterozoic Svecofennian domain of the Fennoscandian Shield (Fig. 1). Refraction measurements were done along the 330 km long profile in 1994 (FENNIA Working Group, 1998).

* Corresponding author. Fax: +358 8 5531414.
E-mail addresses: Kari.Moisio@oulu.fi (K. Moisio), Pertti.Kaikkonen@oulu.fi (P. Kaikkonen).

0264-3707/$ – see front matter © 2004 Elsevier Ltd. All rights reserved.
doi:10.1016/j.jog.2004.06.003

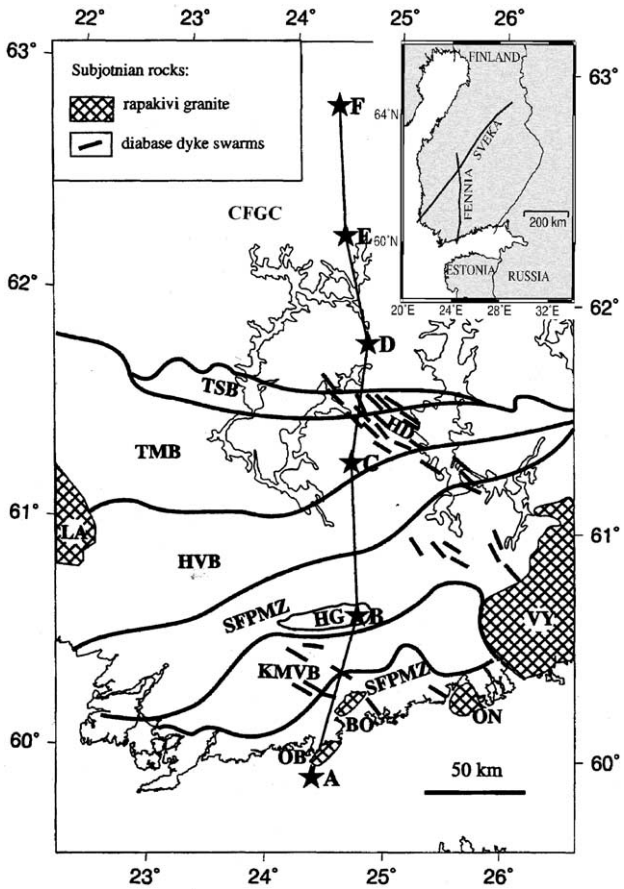

Fig. 1. Geological units in the vicinity of the FENNIA profile (after Koistinen et al., 1996). CFGC, Central Finland Granitoid Complex; TSB, Tampere Schist belt; TMB, Tonalite Migmatite belt; HD, Häme diabase dyke swarm; HVB, Häme Volcanic belt; SFPMZ, Southern Finland Potassium Migmatite zone; KMVB, Kemiö–Mäntälä Volcanic belt; HG, Hyvinkää Gabbro. Rapakivi batholiths: VY, Vyborg; LA, Laitila; OB, Obbnäs; BO, Bodom; ON, Onas. Letters A–F along the FENNIA profile refer to the shot points (modified from FENNIA Working Group, 1998).

Among the first rheological studies for the Fennoscandian Shield was a paper by Cloetingh and Banda (1992) in the European Geotraverse project. Dragoni et al. (1993) presented more extensive analysis of the rheological structure in the Fennoscandian Shield, which was specified in Pasquale et al. (2001). For the central Fennoscandian Shield rheological conditions were presented in Kaikkonen et al. (2000). These studies have shown that rheologically there is a clear distinction between areas of different ages. For example, the brittle–ductile transition depth is largest in the old Archaean area. Further, consequences of the obtained rheology have been studied in the two-dimensional finite-element models (Moisio et al., 2000; Moisio and Kaikkonen, 2001) where responses of the lithospheric structural models were studied.

In this paper we utilize the seismic model of the FENNIA profile to calculate a thermal and rheological model in two dimensions and further to derive resulting stress and deformation using the finite-element

method. This technique is essentially similar as in Moisio et al. (2000) and Moisio and Kaikkonen (2001) with some modifications, which will be discussed in the following text. We also analyse the possible effects of the temperature in the rheology and structural models with uncertainty analysis.

2. Geological and geophysical background

2.1. Geology

The DSS profile FENNIA runs in S–N direction in the Proterozoic terrain, which was mainly formed during the Svecofennian orogeny (1.9–1.8 Ga). This orogeny created the anomalously thick crust, which characterises the central Fennoscandian Shield. The last major tectonic activity after the orogeny produced anorogenic rapakivi granites (1.65–1.54 Ga) in southwest and southeast Finland (Haapala and Rämö, 1992). The FENNIA profile (Fig. 1) transects metavolcanic (e.g. the Tampere Schist belt), metasedimentary (the Tonalite Migmatite belt) and late-orogenic plutonic (the Southern Finland Potassium Migmatite zone) belts ending in the synorogenic Central Finland Granitoid Complex (CFGC), which is a large granitic intrusion. These features are assumed to represent traces of two major collisions during the orogeny (Nironen, 1997). The CFGC is considered to have formed by subduction of the oceanic crust beneath the Proterozoic crust (Korsman et al., 1999). For detailed description of the evolution of the Fennoscandian Shield and the Svecofennian domain see, e.g. Gaal and Gorbatschev (1987) and Windley (1992).

2.2. Geophysical data

The seismic model of the FENNIA (Fig. 2) was constructed from refracted and reflected P- and S-waves (FENNIA Working Group, 1998). The model shows low velocity gradients and small velocity contrast at the seismic boundaries and typical results for the crustal thickness in the central Fennoscandian Shield. The largest Moho depth of 61 km is found in the central part of the profile. The crust is only 48 km thick in the southern part of the profile where also a significant gradient in the crustal thickness is found. In the northern part the crust is approximately 57 km thick. In the seismic velocity model the upper crust is divided into three layers and it has the P-wave velocities between 5.9 and 6.3 km/s and the thickness around 20 km. The middle crust has velocities between 6.45 and 6.7 km/s at a depth from 20 to 30 km. The smallest velocities in this layer are found in the southern part of the profile. The lower crust has the largest thickness variation and also most of the crustal thickness variations along the FENNIA profile. The P-wave velocities in the lower crust are between 6.9 and 7.5 km/s. The smallest depth range in the lower crust is between 30 and 48 km, i.e. the thickness of 18 km and the largest is from 30 to 61 km, i.e. 31 km. In the Moho the P-wave velocities along the profile vary between 8.25 and 8.38 km/s. The ratio of P- and S-wave velocities is 1.69–1.70 in the upper crust and 1.76 in the middle and lower crust.

Surface heat flow density (HFD) measurements in the Fennoscandian Shield are reported, e.g. by Kukkonen (1988, 1993) and particularly in the central part of the Shield by Kukkonen (1998). The FENNIA profile is located in an area where quite high HFD values, i.e. nearly 70 mW m^{-2} have been measured in the nearby drill holes. On the other hand values below 40 mW m^{-2} have been measured under a distance of 100 km from these high HFD drill holes. Generally, a small decrease in HFD is

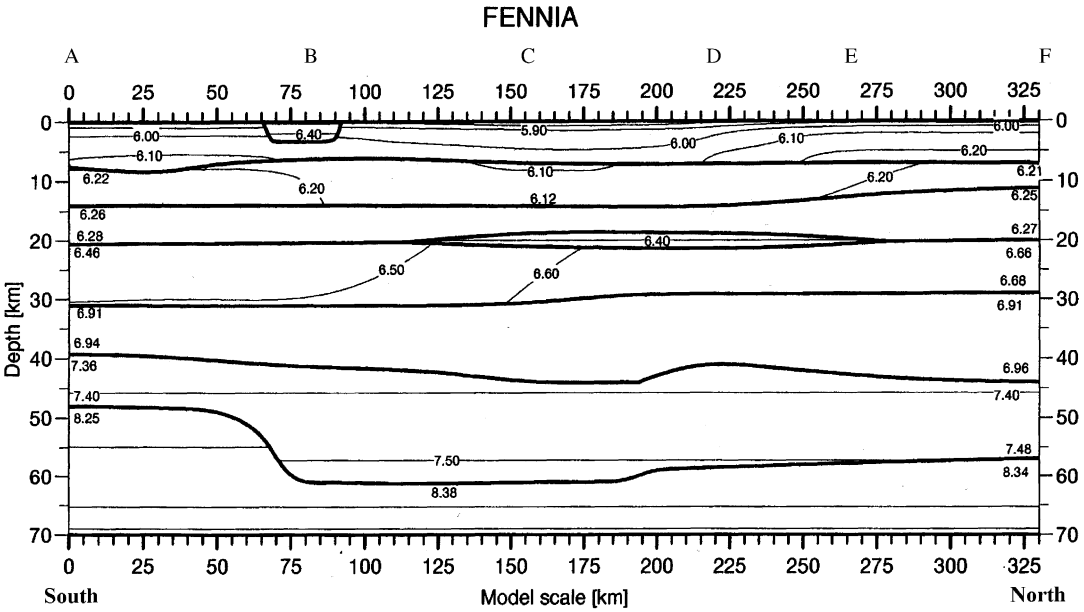

Fig. 2. The two-dimensional velocity model of the crust along the FENNIA profile (FENNIA Working Group, 1998). Thick lines are layer boundaries and thin lines velocity isolines.

observed when moving towards the north. Overall HFD values vary between 40 and 45 mW m^{-2} along the profile. The measured radiogenic heat production values in the central Fennoscandian Shield are discussed for example in Kukkonen (1989, 1993). Surface values are in maximum around 3 μW m^{-3}. In the CFGC area mean value of 1.6 μW m^{-3} has been measured from outcrop samples (Kukkonen and Lahtinen, 2001). Geothermal modelling has been widely applied to the Fennoscandian Shield. The two-dimensional thermal model of the SVEKA transect (Kukkonen, 1998), which is located in the vicinity of the FENNIA profile (Fig. 1) provides valuable information in the form of thermal material parameters.

Thickness of the lithosphere in the Fennoscandian Shield has been estimated from different geophysical measurements and analysis, e.g. from seismic surface wave and P-wave residual analysis (Calcagnile, 1982; Babuska et al., 1988), from seismic tomography analysis (Sandoval et al., 2004) and from xenolith data (Kukkonen et al., 2003). Earlier analyses estimated the lithosphere thickness to be about 180–190 km while the latest results indicate thicker lithosphere with values around 250 or even 300 km.

In situ stress data for Finland is available in few sites. Values of over 40 MPa have been measured for the maximum horizontal stress (Klasson and Lejon, 1990; Saari, 1992) in the NW–SE direction, which corresponds with dominating compressional stress conditions, reported by Chen (1991) and Kakkuri (1997).

An earthquake activity in Finland is generally quite low and also the magnitudes of the earthquakes are relatively small (Ahjos and Uski, 1992). In southern Finland the number of earthquakes is very small, therefore earthquake data cannot be directly used for the DSS profile FENNIA. Focal depth data show that most of the events in the central Fennoscandian Shield occur at a depth smaller than 15 km. For more details see, e.g. Kaikkonen et al. (2000).

3. Modelling

3.1. Background theory

The rheological strength is defined as a difference between maximum and minimum principal stresses and it gives the stress difference required for the rock to deform either in a brittle or in a ductile manner. The brittle strength is described by a frictional shear failure criterion (Byerlee's law), which can be expressed as (see, e.g. Ranalli, 1995).

$$\sigma_1 - \sigma_3 = \alpha\rho g z(1 - \lambda), \tag{1}$$

where ρ is the density, g is the gravitational acceleration, z is the depth, λ is the hydrostatic pore fluid factor (ratio of pore fluid pressure to overburden pressure) and α is a parameter depending on the fault type. We have used a value $\alpha = 3$, which is a result of a friction coefficient value of 0.75 for thrust (compressional) faulting. The upper crust is quite often assumed to have some amounts of water occupying the pore space. A pore fluid pressure reduces the strength required for fracturing and an assumption of a hydrostatic pore fluid pressure is made by applying a pore fluid factor $\lambda = 0.35$.

The ductile strength can be described with the ductile flow law, i.e. the creep law, from which the power law (Eq. (2)) and the Dorn law (Eq. (3)) relations are used (Goetze and Evans, 1979; Carter and Tsenn, 1987; Ranalli, 1995). The flow law gives the stress difference necessary to achieve a given strain rate

$$\sigma_1 - \sigma_3 = \left(\frac{\dot{\varepsilon}}{A_\mathrm{p}}\right)^{1/n} \exp\left(\frac{E_\mathrm{p}}{nRT}\right), \tag{2}$$

$$\sigma_1 - \sigma_3 = \sigma_\mathrm{D}\left[1 - \left(-\frac{RT}{E_\mathrm{D}} \ln\left(\frac{\dot{\varepsilon}}{A_\mathrm{D}}\right)\right)^{1/2}\right] \tag{3}$$

where A_p, n and E_p are the empirically determined material parameters for the power-law (see Table 1), T is the temperature, $R = 8.314\,\mathrm{J\,mol^{-1}\,K^{-1}}$ (universal gas constant) and $\dot{\varepsilon}$ is the strain rate. We have used a uniform strain rate of $\dot{\varepsilon} = 1 \times 10^{-15}\,\mathrm{s^{-1}}$ in all of our calculations. At higher stresses (>200 MPa) for olivine mineralogy the Dorn law is used instead of the power law. In the ductile regime also assumption of whether rock is dry or wet is made upon creep parameters. Hydrous environments can possibly occur in the crust and the mechanism of hydrolytic weakening reduces the ductile strength considerably.

In thermal modelling we have taken into account the temperature dependence of the thermal conductivity following the relationship in Eq. (4).

$$k(T) = k_\mathrm{ref}\left[\left(\frac{1}{1 + bT}\right) + c(T + 273.15\,\mathrm{K})^3\right] \tag{4}$$

where T is the temperature (°C), k_ref is the conductivity at the room temperature ($\mathrm{W\,m^{-1}\,K^{-1}}$) and b and c are empirical constants ($b = 0.0015\,\mathrm{K^{-1}}$, $c = 1 \times 10^{-10}\,\mathrm{W\,m^{-1}\,K^{-4}}$).

Table 1
Material parameters and the petrology used in geothermal and rheological calculations (from Carter and Tsenn, 1987; Wilks and Carter, 1990; Ranalli, 1995; Kukkonen, 1998)

Layers	Petrology	Power law exponent, n	Activation energy, E_p (kJ mol^{-1})	Initial constant, A_p (MPa^{-n} s^{-1})	Thermal conductivity, K (W m^{-1} K^{-1})	Heat production, A (μW m^{-3})	Density, ρ (kg/m^3)
Upper and middle crust	Granite (wet)	1.9	140	2.0E − 04	3.0	2.0–0.5	2650–2850
	Diorite (wet)	2.4	212	3.2E − 02	3.0	0.4–0.3	2800–2850
	Granite (dry)	3.3	187	2.0E − 06	3.0	0.4–0.3	2800–2850
Lower crust	Mafic granulite (dry)	4.2	445	1.4E + 04	3.0	0.2–0.1	2870–2950
Mantle	Olivine (dry)	3.0	510	7.0E + 04	4.2	0.05–0.002	3100–3800

Flow parameters for the Dorn law

	Petrology	Activation energy, E_D (kJ mol^{-1})	Initial constant, A_D (s^{-1})	Dorn law stress, σ_D (GPa)			
Mantle	Olivine	535	5.7E + 11	8.5	4.2	0.05–0.002	3100–3800

Table 2
Lithology used in the strength calculations for creep laws

	Dry	Wet
Upper crust	Granite	Granite
Middle crust	Granite	Diorite
Lower crust	Mafic granulite	Mafic granulite
Mantle	Olivine	Olivine

3.2. Model parameters

The two-dimensional thermo-structural model for the FENNIA profile is constructed using the seismic P-wave velocity model (Fig. 2) as a basis for the structural model, i.e. the velocity boundaries define the structural boundaries where material properties, e.g. density, change. We have divided the crust in the same manner as in the seismic velocity model, i.e. the upper, middle and lower crust. Furthermore we have added a lithospheric mantle and an upper part of the asthenosphere. Thickness of the lithosphere is based on seismic surface wave and P-wave residual analysis (Calcagnile, 1982; Babuska et al., 1988) and it is approximately 180 km at the southern edge of the model slightly dipping towards the north where the thickness is 190 km.

Elastic material parameters are taken from Carmichael (1989) for typical rock types occurring in the Proterozoic Fennoscandian crust. Also the ratio of P- and S-wave velocities is used to confine the Poisson's ratio. Densities (Table 1) increase as a function of depth in the model, but inside the defined areas they are constant. The values of density are adapted from the seismic model and also the gravity model of Kozlovskaya and Yliniemi (1999) is used as a guideline. Rheological parameters (Table 1) are taken from Carter and Tsenn (1987), Wilks and Carter (1990) and Ranalli (1995). A paper by Fernàndez and Ranalli (1997) compiles upper and lower crustal and also upper mantle ductile creep parameters from several authors. Lithological model of the DSS profile SVEKA (Kukkonen, 1998) derived from P- and S-wave velocities and the compilations of seismic properties (Holbrook et al., 1992; Rudnick and Fountain, 1995) together with the data from the FENNIA profile makes it possible to use probable creep parameters in the middle and the lower crust. For the wet crustal conditions we have used creep parameters of the wet granite and wet diorite in the upper and middle crust, respectively, and for the dry conditions dry granite has been used both in the upper and middle crust. For the lower crust the parameters of the mafic granulite and for the mantle the parameters of olivine are used both for the wet and dry models (Table 2). The geothermal parameters (Table 1), i.e. values of the thermal conductivity and the heat production are mainly from Kukkonen (1998). For the northern part of the profile, i.e. the CFGC area, measured heat production values and the model for the lithospheric heat production (Kukkonen and Lahtinen, 2001) are also used as constraints. In the uppermost crust the heat production has maximum values of 2.0 $\mu W\,m^{-3}$ while the lower crust has values of 0.1–0.2 $\mu W\,m^{-3}$. The heat production is assumed to be constant inside the defined areas.

3.3. Modelling procedure

The finite-element model is 300 km long and 250 km deep and it consists approximately of 28,000 elements and 24,300 nodes. In the crust the largest vertical size of the element is around 1.5 km while in

the Moho this size it is about 1 km from where it slowly increases to 5 km at the base of the model. The horizontal size is about the same in the crust but in the mantle slightly higher around 4–5 km. Vertical size defines also the resolution for the strength calculations. The thermal boundary conditions are a constant temperature of 5 °C at the surface of the Earth and of 1100 °C at the lower boundary, i.e. at the lithosphere–asthenosphere boundary, which is assumed to follow the solidus of ultramafic rocks. The thermal finite-element model is solved assuming two-dimensional conductive steady-state conditions. The solved temperature is furthermore used in the rheological calculations to derive the ductile strength and along with the brittle strength these values are taken into the structural finite-element model as elastoplastic non-linear material parameters. The structural model has the same geometry and element distribution as the thermal model.

The boundary condition of 50 MPa compressional pressure simulating tectonic contribution of the stress field is applied to the northern vertical edge of the model. This value is chosen by comparing trial and error results with the measured stress field values (Saari, 1992). With this value our modelling derives in reasonable stress field intensity. Modelling results are however very difficult to verify with the measured values as the number of the measurements is quite low. The orientation of the model (N–S) in comparison with the direction of maximum horizontal stress in Finland (NW–SE) is not ideal but in a two-dimensional model only possible procedure. This is a restriction we have to accept, as otherwise it would require three-dimensional modelling for proper orientation. Gravitational effects are neglected, i.e. only the deviatoric state of the stress is studied. The structural model is solved with the finite-element method assuming a plane strain approach (2-D), i.e. the displacement (and also an equivalent strain) in one direction is zero. All finite-element calculations were done with the software package ANSYS^{TM}.

4. Results and discussion

4.1. Thermal model

The temperature varies approximately from 470 to 440 °C from S to N at the depth of 50 km (Fig. 3a). The thermal model used is labelled as $T = 1100$ °C and from this point forward is referred as the reference model as it is the principal model used in this paper. Lowest temperature values are found in the northern part of the profile, i.e. in the CFGC area. The HFD (Fig. 3b) changes only slightly at the 50 km level, where still mainly exists lower crustal material. The minimum values are around 12.5 mW m^{-2} and the maximum ones at 13.3 mW m^{-2}. In the mantle the HFD is quite constant with small variation between values of 11 and 12.5 mW m^{-2} while at the surface of the Earth these values (Fig. 3b) range from 46 to 38 mW m^{-2}. These values correspond well with earlier thermal modelling done for the region and with the measured surface HFD values. In comparison with the results of Moisio et al. (2000) and Moisio and Kaikkonen (2001) there are some variation. This is a consequence of different boundary conditions used and especially the temperature dependence of thermal conductivity has quite significant influence particularly on the mantle.

4.1.1. Uncertainty analysis

The temperature is an important factor in the rheological modelling. However, large uncertainties are connected to the temperature estimation in the deep lithosphere. The surface HFD is evaluated from the temperature measurements in the deep boreholes and these measurements themselves can contain errors,

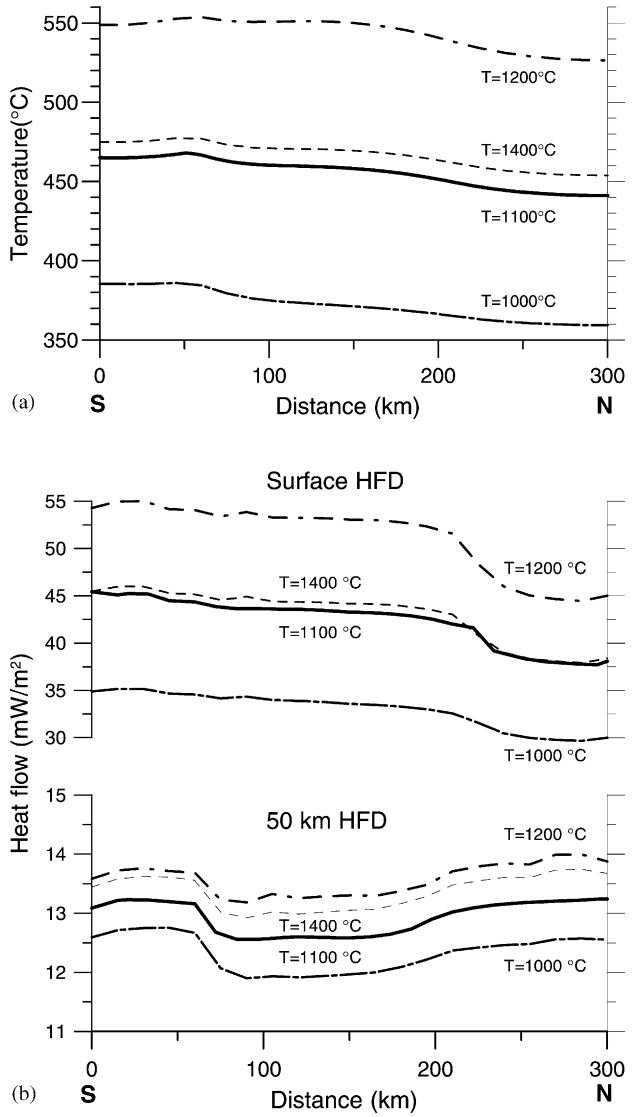

Fig. 3. (a) The temperature at the depth of 50 km along the FENNIA profile for the four thermal models (T = 1000, 1100, 1200 and 1400 °C). The reference model used is displayed by the thickest line and with the label T = 1100 °C. Other three models are labelled with corresponding temperature value. (b) The heat flow density (mW m^{-2}) at the surface of the Earth (upper axis) and at the depth of 50 km (lower axis) for the four thermal models along the profile. Note that the scale is different between the two axes.

for example, groundwater circulation and topography bias measured values. Furthermore, the location of the HFD measurements cannot usually be chosen randomly resulting in unevenly distributed and possible large distances between measurement sites. In general variation in the surface HFD with an amount of $\pm 10\,\mathrm{mW\,m^{-2}}$ changes the temperature in the depth of 50 km approximately $\pm 100\,^{\circ}\mathrm{C}$. Petrophysical parameters required in the lithospheric thermal modelling, namely the thermal conductivity and the heat

production, can only be estimated indirectly from geophysical measurements except for the uppermost crust. Deep seismic soundings are conventionally used for estimating the petrology of the lithosphere. This evidently leads to more or less erroneous values for the petrophysical parameters needed. Thermal conductivity varies usually between values of 2 and 4 $W\,m^{-1}\,K^{-1}$ while heat production can vary between several decades (Kukkonen, 1998) from the low values in the mantle to the high values in the upper crust. The combined effect when both parameters vary can result in a similar amount of change in the temperature at the depth of 50 km as caused by the change in the surface HFD by $\pm 10\,mW\,m^{-2}$ (Jokinen and Kukkonen, 1999).

Possible errors in temperature estimation are analysed with two different thermal models, where rather high temperature difference compared to the reference model is generated. The first variant is calculated with lower heat production in the crust and a lower temperature of 1000 °C in the lithosphere–asthenosphere boundary. Just the opposite is done for the second variant where the crust has higher heat production and a higher temperature of 1200 °C in the lower boundary. These two variants are displayed in Fig. 3a and b and distinguished with corresponding temperature labels. In general these variants result in a temperature difference of the order of ±100 °C in the depth of 50 km (Fig. 3a). Surface HFD values in the low temperature model are approximately 10 $mW\,m^{-2}$ lower and in the high temperature model as much higher in the level of 50 km (Fig. 3b). The difference in the HFD in comparison with the reference model at the same depth is close to $\pm 0.5\,mW\,m^{-2}$ for both models.

Furthermore, a third model variant is calculated where the temperature in the lithosphere-asthenophere boundary is raised to 1400 °C (Kukkonen and Peltonen, 1999). Also the boundary itself is shifted 50 km deeper to the level of 240–250 km to simulate the thick lithosphere in the Fennoscandian Shield as recently suggested by, e.g. Kukkonen et al. (2003) and Sandoval et al. (2004). Results show that the temperature (Fig. 3a) in this model is however quite close to the values of the reference model as the difference is approximately only 10 °C in the depth of 50 km. The HFD values in the surface are practically the same as in the reference model and in the depth of 50 km a small difference, lower than $0.5\,mW\,m^{-2}$, is observed.

The percentage of difference in the temperature between the reference model (T = 1100 °C) and the temperature model variants (T = 1000, 1200 and 1400 °C) as a function of depth is shown in Fig. 4. This difference is shown for three locations along the FENNIA profile where these points are the same as in Fig. 5, i.e. 0, 100 and 300 km. A maximum difference is found in the crust being approximately 20% higher (T = 1200 °C) or lower (T = 1000 °C) than the reference value. A small difference of a few percents can be distinguished between different locations in the crust. In the mantle difference is in minimum below 10% and not so dependent on the location. In the thick lithosphere model (T = 1400 °C) temperature is only few percents higher than the reference value in all of the three locations.

4.2. Structural model

The calculated rheological strength with wet upper and middle crust for the FENNIA profile (Fig. 5) results in a layered structure where quite thin rheologically weak layers are present. These weak layers are the possible areas for deformation to occur. There is a minimum in the upper crust between the depths of 15 and 20 km and in the middle crust between 25 and 30 km. The upper crustal minimum reaches the lowest strength values. These weak layers are separated by a maximum in the strength. A maximum is also found in the upper part of the lower crust, between the depths of 38 and 44 km resulting from the lower crustal layer of ‘strong’ mafic granulite. Downwards from this depth the ductile strength decreases until it reaches the Moho boundary. Only at the thickest part of the crust (∼61 km) the strength has values

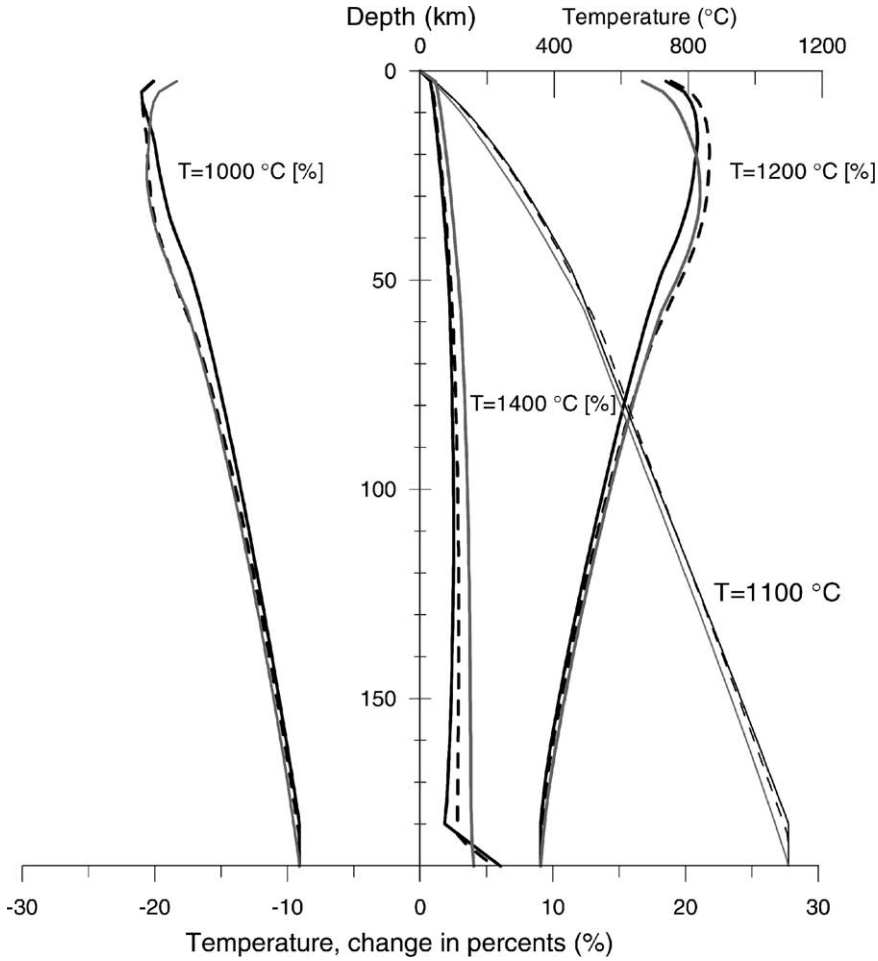

Fig. 4. Geotherms for the reference model (T = 1100 °C) in three locations; 0 km (dark solid line), 100 km (dashed line) and 300 km (light solid line) and the percentage of difference between the reference model and the three thermal models T = 1000, 1200 and 1400 °C in the same locations. Note that the temperature scale is valid only for the geotherms, i.e. the graphs labelled with T = 1100 °C.

low enough to necessitate in a significant deformation. In the mantle the strength reaches significantly low values approximately at the depth of 110 km. These main features are more evident in the attached strength envelope presentations from three locations along the profile (Fig. 5). These locations are the same as used in Fig. 4. The maxima define the brittle–ductile transitions from which the upper crustal maximum can be considered to be more important. This transitional layer is located between the depths of 11 and 14 km. The middle crustal maximum is located between 20 and 24 km.

Typically the brittle–ductile transition is considered to be the lower limit of the earthquake focal depths. However, the real lower boundary of the seismicity is controlled by modification of the frictional behaviour. This transition between velocity-weakening and velocity-strengthening for granitic composition is approximately at the temperature of 350 °C (Scholz, 1990; Blanpied et al., 1991). In our thermal model the depth of 350 °C appears between 34 and 37 km from south to north, respectively. This transitional depth

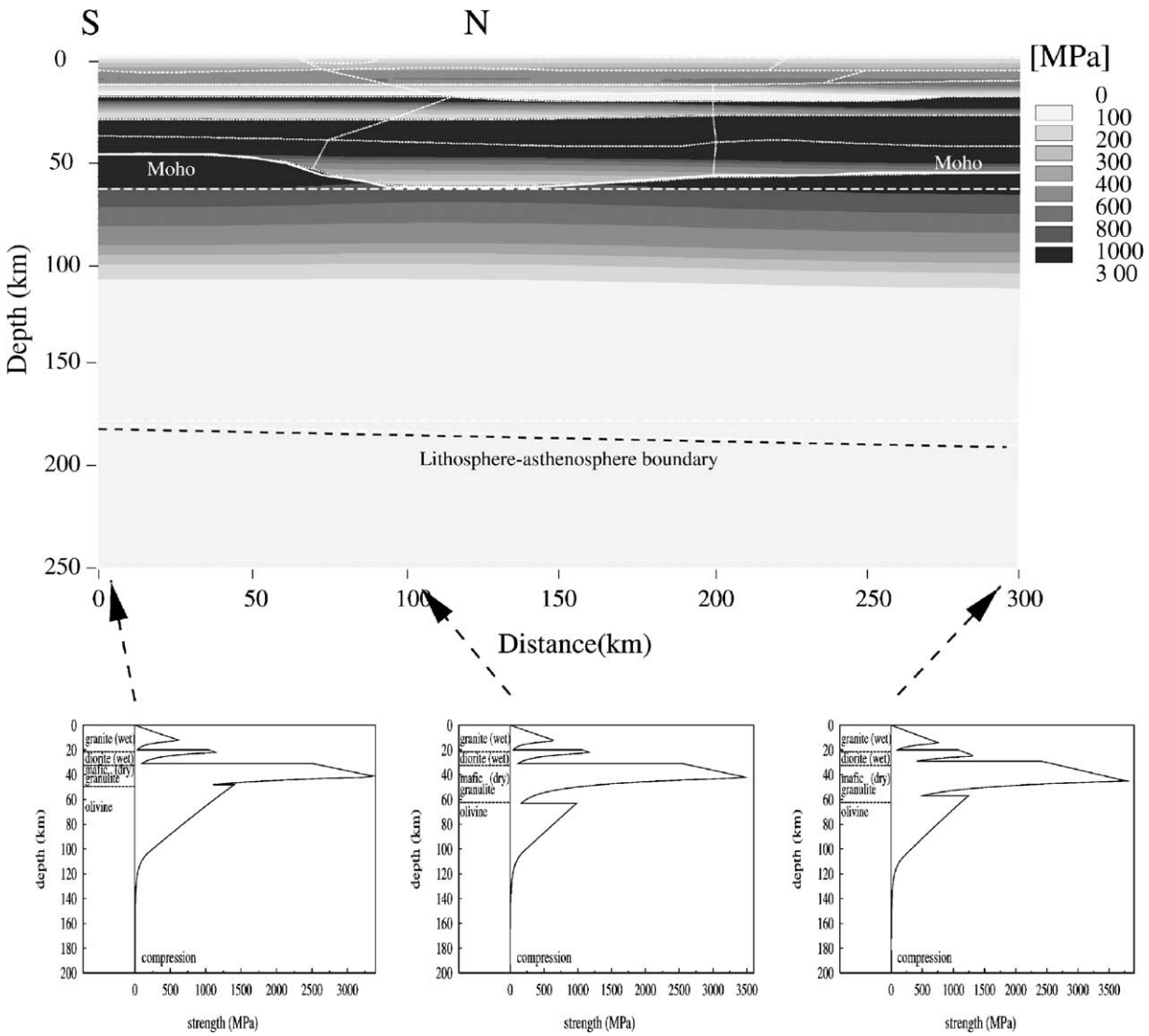

Fig. 5. The rheological strength (MPa) of the wet model for the FENNIA profile. Lithology is wet granite and diorite in the upper and middle crust, respectively, dry mafic granulite for the lower crust and olivine for the mantle. Note that the contour levels are not uniform and horizontal and vertical scales are not the same. The strength envelopes below are shown for three locations in the profile: 0, 100 and 300 km.

is much larger than the brittle–ductile transition depth derived from our model. Analysis of the focal depth distribution in the central Fennoscandian Shield has shown that 99% of the events occurred above the depth of 31 km and 80% above the depth of 14 km (Kaikkonen et al., 2000). Focal depth data (Ahjos and Uski, 1992) shows that the highest occurrence of the events is in the upper crust but it should be noted that the data used in Kaikkonen et al. (2000) covers approximately whole Finland whereas our model is located in the southern Finland. It seems that the rheological model for the FENNIA profile correlates to some extent

with the earthquake data in the central Fennoscandian Shield. On the other hand the depth of 350 °C temperature derived from our thermal model would allow also deeper earthquakes according to the definition above.

For the low and high temperature models (T = 1000 and 1200 °C) the depth of the 350 °C isotherm is between 44–48 and 26–30 km, respectively. The depth range of 44–48 km is slightly too deep in comparison with the focal depth data, while range of 26–30 km fit better with the focal depth.

Dry rheological conditions have a major impact on the rheology, both on the brittle and ductile behaviour. In the brittle regime an assumption of the dry conditions increases the strength as the pore fluid factor is neglected. In the ductile regime the consequences are similar, i.e. the ductile strength increases as the material becomes stronger. The rheological strength for the dry crust is shown in Fig. 6 where a clear difference in the rheological structure in comparison with the wet conditions is found. A layered structure is simpler with upper crustal maximum and middle crustal minimum. The lower crust and the mantle have the same material parameters as in the wet model so they show the similar features as earlier. The dry brittle–ductile transition is between depths of 19 and 22 km. This is also in agreement with the focal depths of the central Fennoscandian Shield. A minimum follows this maximum with lowest values at the boundary of the middle and the lower crust at the depths of 29–31 km.

In this paper principal stresses are treated so that $\sigma_1 > \sigma_2 > \sigma_3$, i.e. σ_1 is the largest and least compressional stress and σ_3 is the smallest and most compressional stress, this is due to the sign convention of negative stresses being compressive used in the modelling program.

The resulting principal stresses for the applied pressure boundary condition of 50 MPa are shown in Figs. 7 and 8. These stresses together with their directions define the state of stress in a point. The first principal stress σ_1 (Fig. 7a) has maximum values of nearly 50 MPa and the direction of the stress field is close to vertical. On the average the values are only around 10–20 MPa as we have neglected the gravity. Most of the maximum values are associated with the northern edge where initial pressure is applied as a boundary condition. Both compressive and tensional stresses are found and overall pure horizontal pressure does not generate very large vertical stresses. The second principal stress σ_2 (Fig. 7b) has maximum values around 30 MPa with most of the stress field being compressional with the direction perpendicular to the profile. The third principal stress σ_3 (Fig. 8a) is the most compressive and has the highest stress values with a maximum above 110 MPa located in the upper mantle approximately at the depth of 100 km. This maximum is an effect of the applied pressure as it is also generated if we change the initial pressure to the southern edge. A significant minimum is found in the uppermost crust between points of 150 and 220 km along the profile. General features of the σ_2 and σ_3 stresses are basically very similar as both of them are horizontal where the direction of the σ_3 stress is nearly parallel to the profile. Principal stresses show how the applied pressure affects in different directions on the structural model with the used rheological conditions.

The stress intensity (Fig. 8b) is defined as the largest difference between absolute values of the principal stresses, in our model typically between σ_1 and σ_3 stresses, and it also gives an indication of the possible areas of failure. The individual principal stresses discussed above already showed the significant features in the stress field that are also seen in the overall stress field, i.e. stress intensity. There is a large maximum in the upper mantle at a depth of about 100 km with a magnitude as large as 120 MPa extending up to the lower crust in the southern part of the profile where the stress values are around 90 MPa. Immediately below the upper mantle maximum a large gradient in the stress field is found where magnitude of the stress intensity drops down to about 30 MPa. This gradient is a consequence of the applied rheological structure where the strength of the mantle has diminished enough to prevent the transmission of the

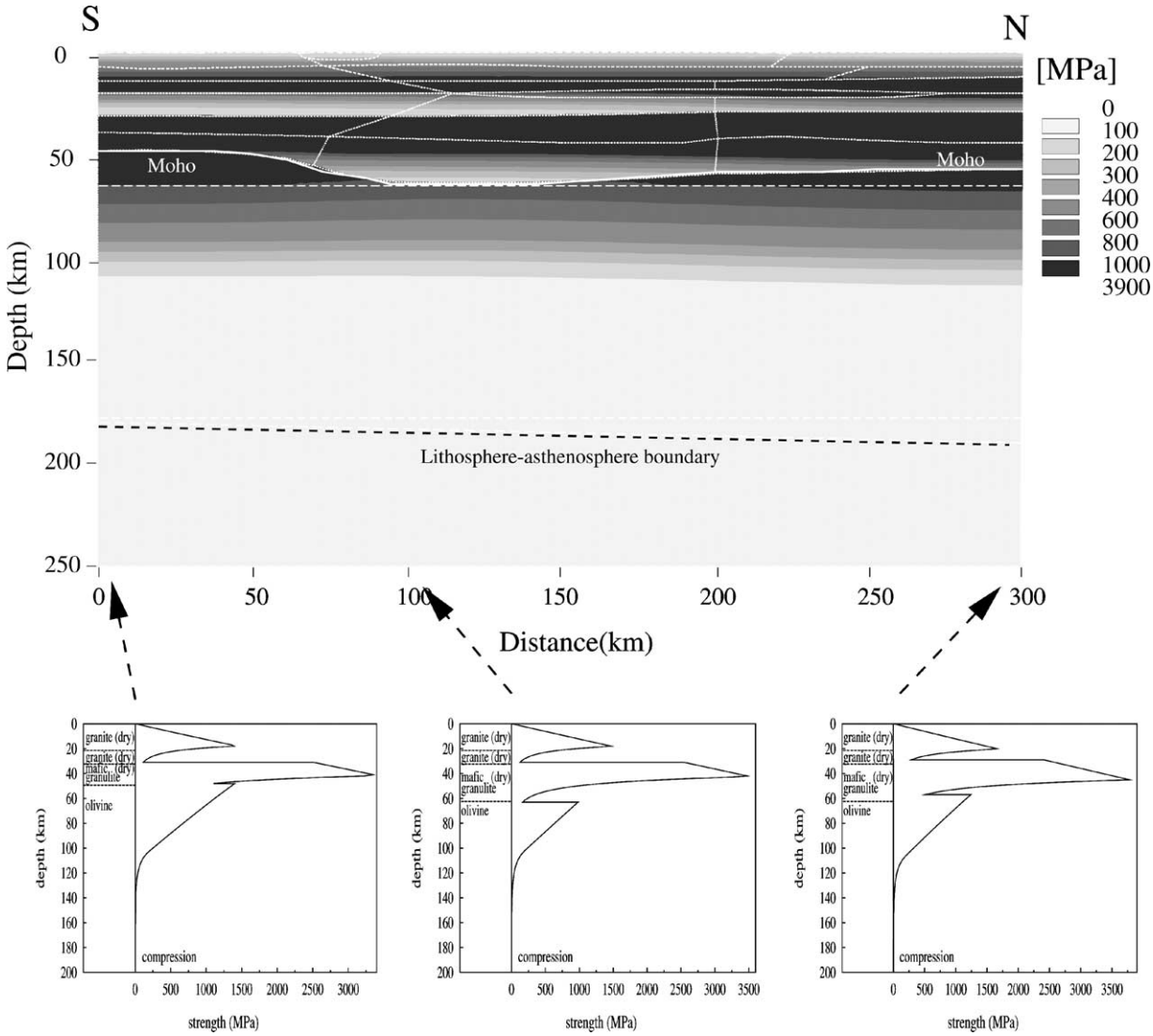

Fig. 6. The rheological strength (MPa) of the dry model for the FENNIA profile. Lithology is dry granite in the upper and middle crust, dry mafic granulite in the lower crust and olivine in the mantle. Note that the contour levels are not uniform and horizontal and vertical scales are not the same. The strength envelopes below are shown for three locations in the profile: 0, 100 and 300 km.

upper mantle stresses down to the mantle. Crustal stress values vary from the largest values of about 90 to 50–70 MPa in the middle crust and 20–50 MPa in the upper crust. Similar minimum as in Fig. 8a is located in the upper crust with magnitude of the stress intensity around 20 MPa. The overall pattern in the stress intensity suggests that these above mentioned features are mainly generated by the applied pressure. However, also the rheological structure used has influence on the stress intensity, especially in the mantle as discussed above. In the crust the effects of the rheology are not clearly distinguished as most of the changes should be concentrated in the weak layers, which are quite thin. A closer look of

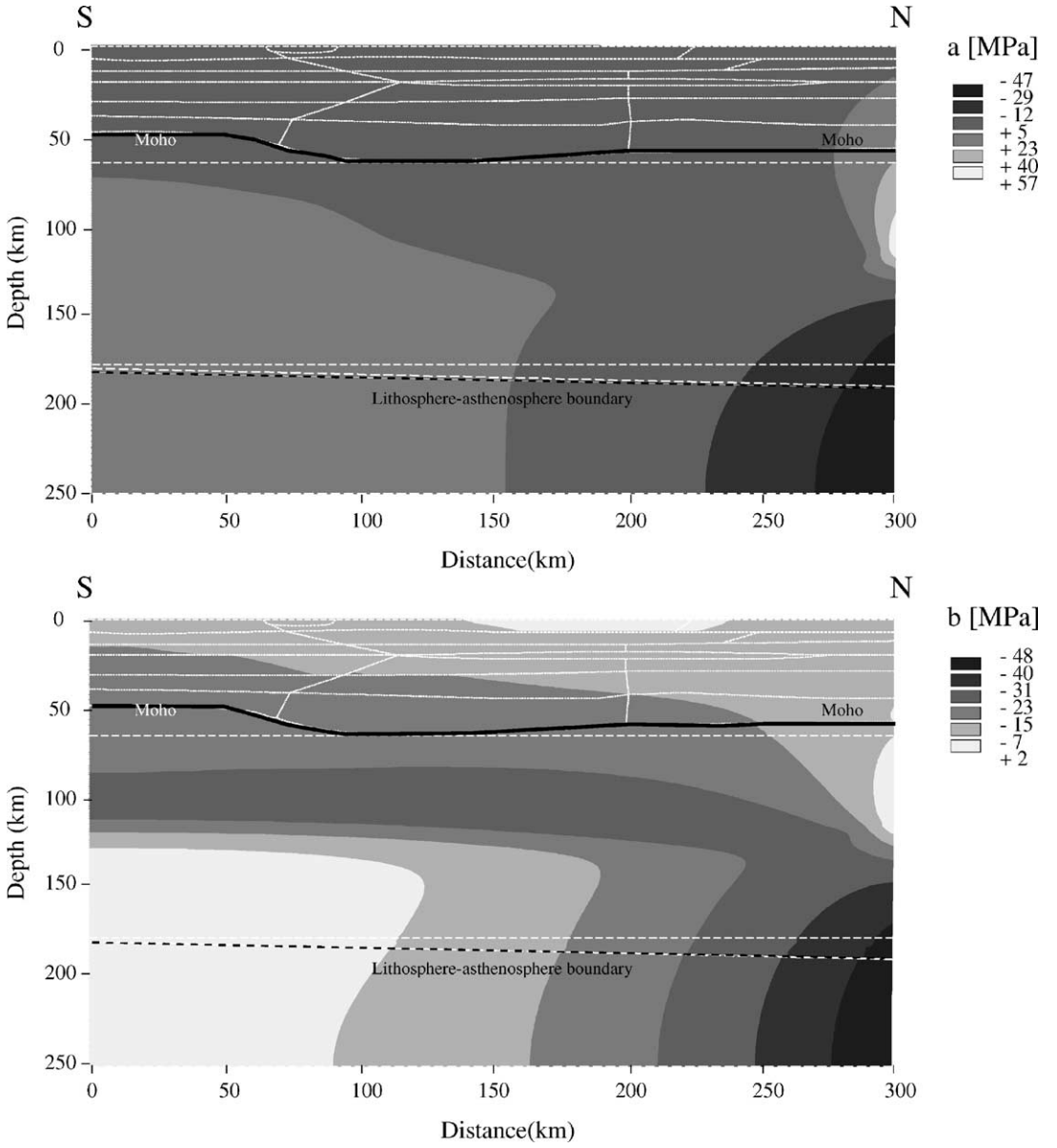

Fig. 7. Magnitude of the first (a) and the second (b) principal stresses σ_1 and σ_2, respectively. Negative values refer to compressional stresses.

the crustal stress intensity shows that a small decrease of about 10 MPa is observed in the rheologically weak zones. It should be noticed that in the northern edge the applied pressure slightly distorts the stress values.

The stress ratio is defined as the ratio between the equivalent stress and the rheological strength and it describes the deviatoric state of stress. It shows areas where brittle or ductile deformation occurs with the stress ratio ≥ 1, i.e. the yield stress is exceeded. Also areas where the stress state is elastic or near failure

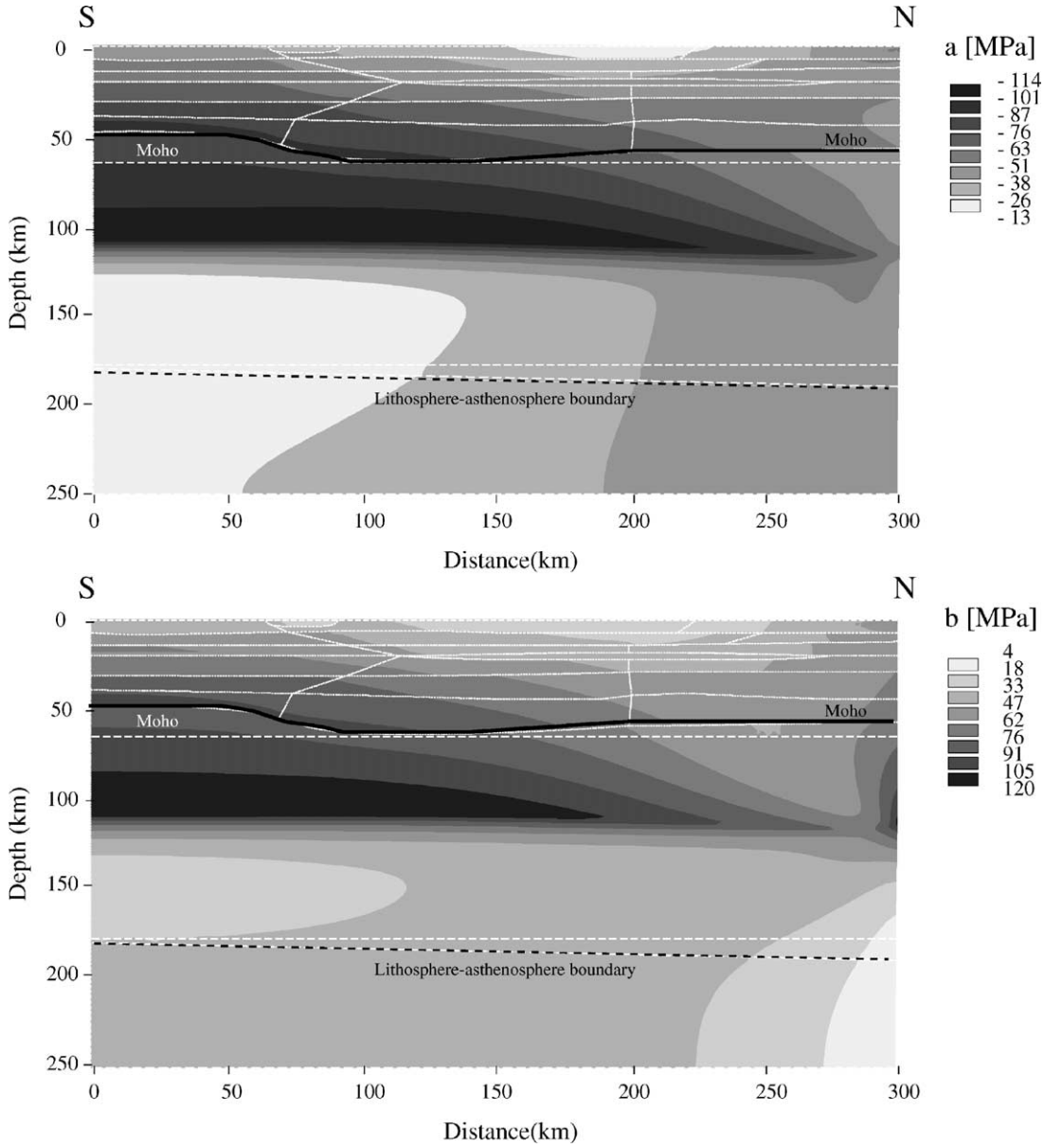

Fig. 8. Magnitude of the third principal stress σ_3 (a) and the stress intensity (b). Negative values refer to compressional stresses.

can be identified. In Fig. 9a the stress ratio for the wet crust is shown for the FENNIA profile where the black colour shows the areas where the stress ratio >1. These areas are found in the mantle and in the boundary of the upper and middle crust where a very thin zone of deformation is found. This crustal zone is a result of the upper crustal strength minimum. A rheologically weaker material or increase in the temperature would create thicker deformational zone, which would have more significant effect on the stress fields in the crust. In the mantle plastic deformation begins around the depth of 100 km. This

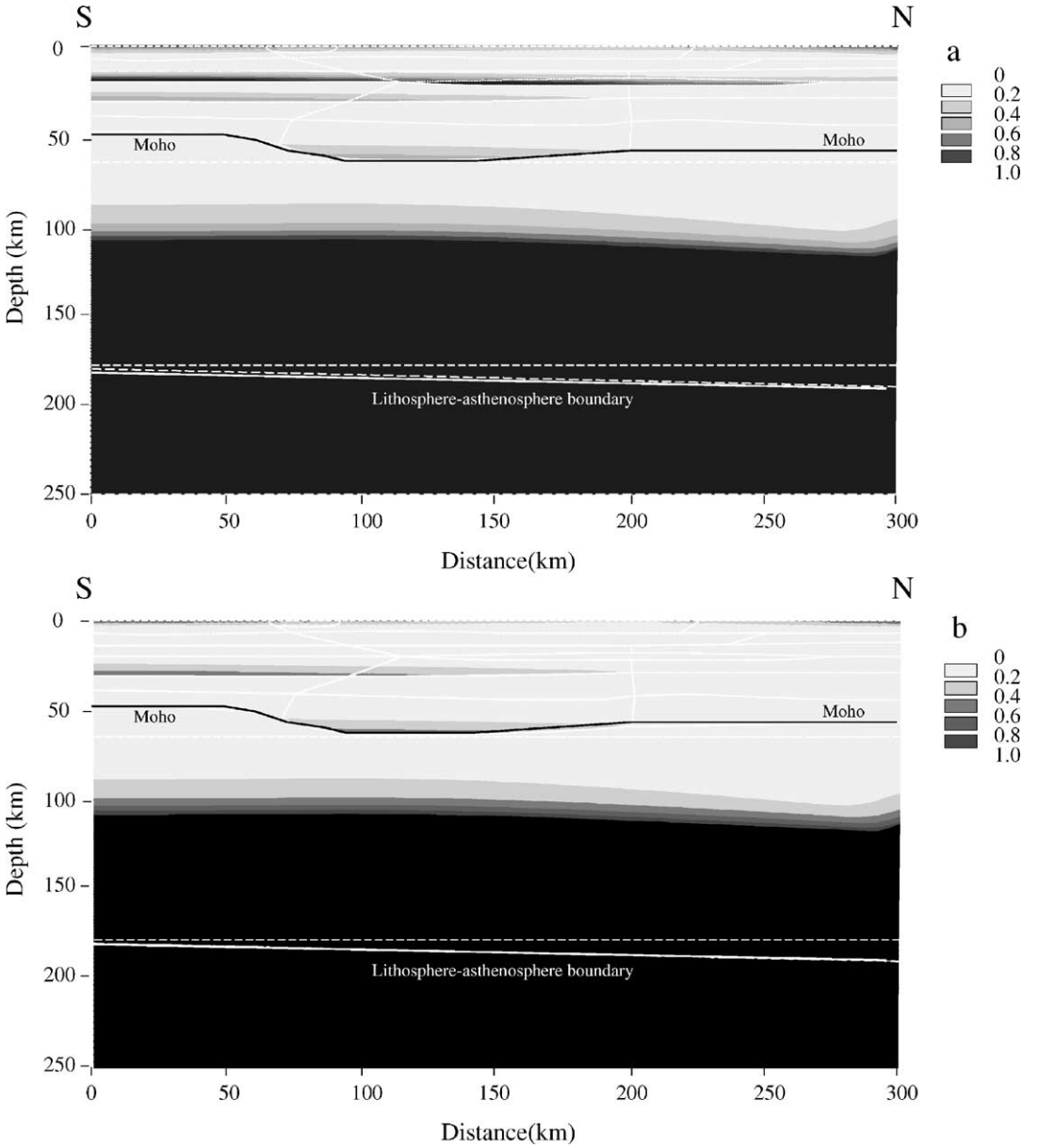

Fig. 9. The stress ratio in (a) the wet and (b) the dry crust shows the yielding areas of the model with ratio higher than one in black colour.

depth is quite constant through the whole profile as it is dominated by the temperature whose variation in the mantle is only few tens of degrees between the edges of the model. In the middle and the deepest part of a crust there are found only a few areas near failure where deformation is possible for example due to increased mechanical loading. The stress ratio for the dry crust is shown in Fig. 9b where a distinct difference can be seen in comparison with the wet crust with no crustal deformation. The dry conditions

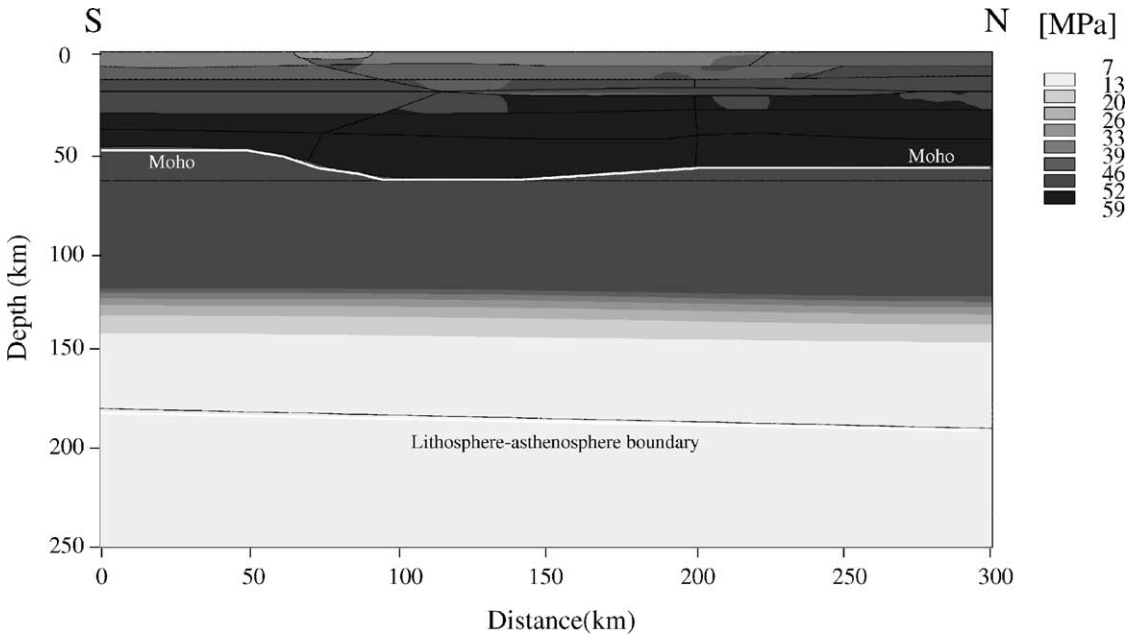

Fig. 10. The stress intensity of the wet model with the displacement boundary condition of 200 m applied to the northern edge.

in the upper and middle crust results in only one very thin zone of deformation in the southern part of the profile.

Initial pressure applied to the model can be considered to resemble the tectonic forces acting on the lithosphere, but as a comparison model with different initial value is calculated. The use of displacement boundary condition of 200 m at the northern edge while southern edge is stationary results in a completely different stress distribution. The largest stresses (Fig. 10) are found in the lower crust with maximum magnitudes close to 60 MPa. In the mantle the stress decreases to very low values at the depth of about 120 km as a result of the low ductile strength. The distribution of the crustal stress field is mainly controlled by material composition. At the surface of the crust the stresses vary between 30 and 40 MPa while in the upper and middle crust they have a range of 40–50 MPa. In the mantle the rheology controls the transmission of the stresses down to the base of the model. Although the stress field is completely different, the deformation, i.e. the stress ratio is almost identical in comparison with the results in Fig. 9. In the mantle a plastic deformation begins slightly deeper due to the lower magnitudes of the stress. In the crust the same thin deformational zone as before is found between the upper and middle crust.

4.2.1. Uncertainty analysis

The temperature estimations can be considered rather important when discussing the errors related to the rheological modelling. In addition, other sources of uncertainties are for example the proper value of the strain rate, rheological parameters, choice of deformation mechanism and whether wet or dry conditions exist. These uncertainties associated with rheological modelling are discussed, e.g. in Fernàndez and Ranalli (1997). In the following we analyse the effect of the temperature in the rheological calculations and furthermore in structural modelling.

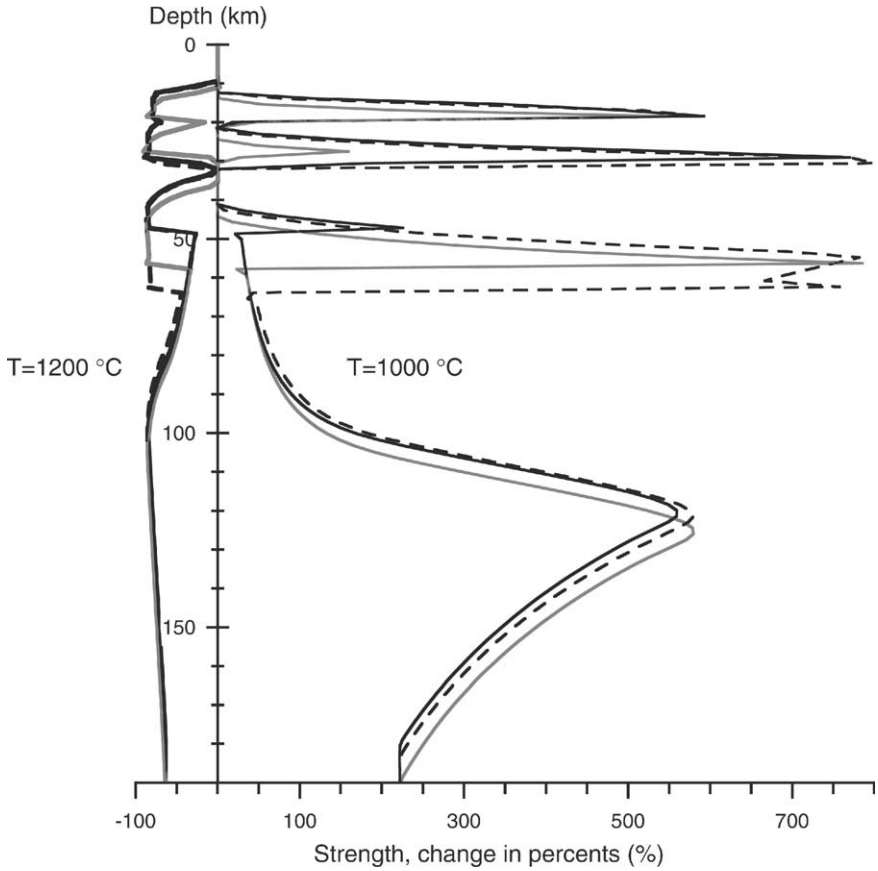

Fig. 11. Percentage of difference in the rheological strength between the model calculated with the reference thermal model (T = 1100 °C) and with the thermal variants (T = 1000 and 1200 °C) for the same locations (0 km, dark solid line; 100 km, dashed line; 300 km, light solid line) as in Fig. 5. Darker lines correspond with the T = 1200 °C model.

How rheological structure and modelling results change due to the different thermal models are analysed by using the previously presented thermal model variants (T = 1000, 1200 and 1400 °C) in comparison with the reference model (T = 1100 °C). Temperature is thereby the only variable affecting the results. In the rheological strength the effects of the temperature are seen in the ductile regions while in the brittle layers there are no differences. Percentage of difference between the rheological strengths calculated with the thermal reference model (T = 1100 °C, see Fig. 5) and the low temperature (T = 1000 °C) and the high temperature (T = 1200 °C) models are shown in Fig. 11 for the same three locations (0, 100 and 300 km) as previously. In the low temperature model, difference is distinct at certain depths, several hundreds percents higher than in the reference model. Highest differences are found in the middle and the lower crust and also in the mantle. These maximum values coincide with the depths where low values of the strength are found in the reference model. In general, the cooler temperature makes the weak ductile regions of the reference model stronger and it also shifts the beginning of the weak regions to deeper depths. For the high temperature model not so radical differences are seen, as the percentage is generally 50–100% lower than in the reference model. Higher temperature reduces the strength, which results in

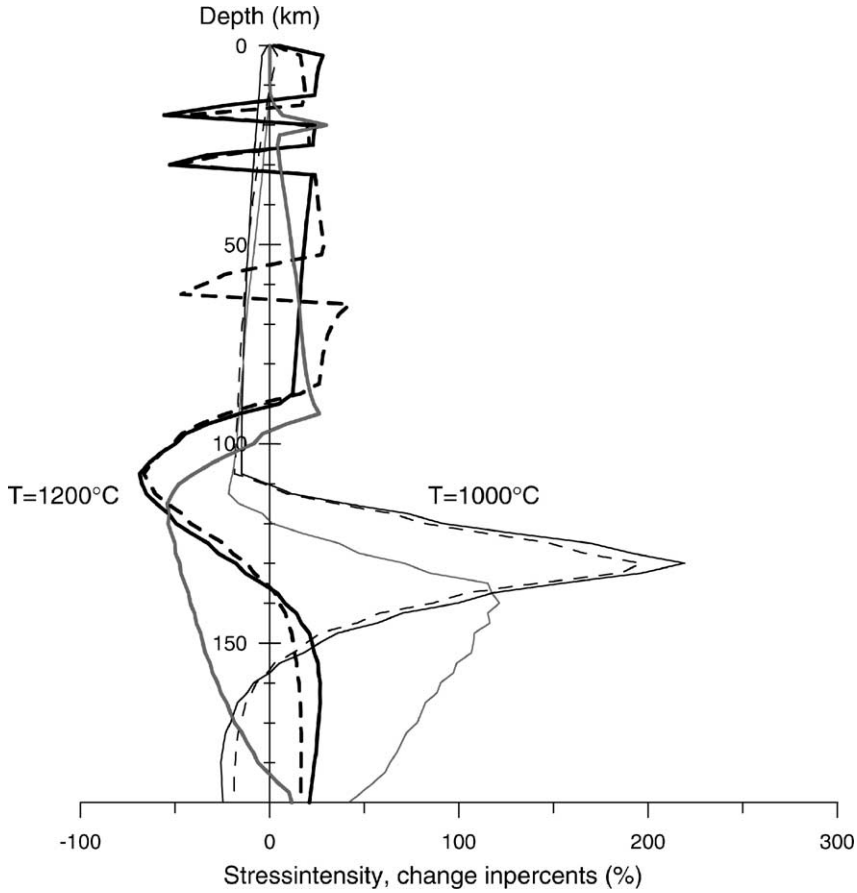

Fig. 12. Percentage of difference in the stress intensity between the model calculated with the reference thermal model (T = 1100 °C) and with the thermal variants (T = 1000 and 1200 °C) for the same locations (0 km, dark solid line; 100 km, dashed line; 300 km, light solid line) as in Fig. 5. Darker lines correspond with the T = 1200 °C model. The values for the 300 km point are disturbed due to boundary condition applied in the same edge.

thicker weak zones in the crust. In the thick lithosphere model (T = 1400 °C) the difference between strength in the crust and upper mantle is mainly around ±10% (not shown) while in the lower mantle it is about 30% lower than the reference model values.

In the stress intensity, percentage of difference (Fig. 12) is more stable for the model with the low temperature (T = 1000 °C) than with the high temperature (T = 1200 °C). In the model with the low temperature the stress intensity is 10–20% lower than in the reference model down to the depth of 110 km where the intensity becomes 100–200% larger than the reference value. This is due to behaviour of the rheological strength (see above) in the mantle where also a large positive percentage was found. In the high temperature model more variation is found in the stress intensity. Noteworthy are the regions in the crust where the stress intensity is about 50% lower than the reference value. These regions coincide with layers of low strength found in the upper and the middle crust. In the graph for the location of 100 km (dashed line in Fig. 12) a reduced value of the stress intensity is also found in the lower crust. A minimum value in the mantle at the depth of 110 km is a result of the lower strength values in the high temperature

model than in the reference model. It should be noted that graphs for the 300 km location (light solid line in Fig. 12) are slightly erroneous as the applied boundary condition distorts them. In the thick lithosphere model (T = 1400 °C) stress intensity has quite low percentage of difference (±10%) down to the depth of 110 km where approximately 20% lower values of the stress are generated (see discussion above).

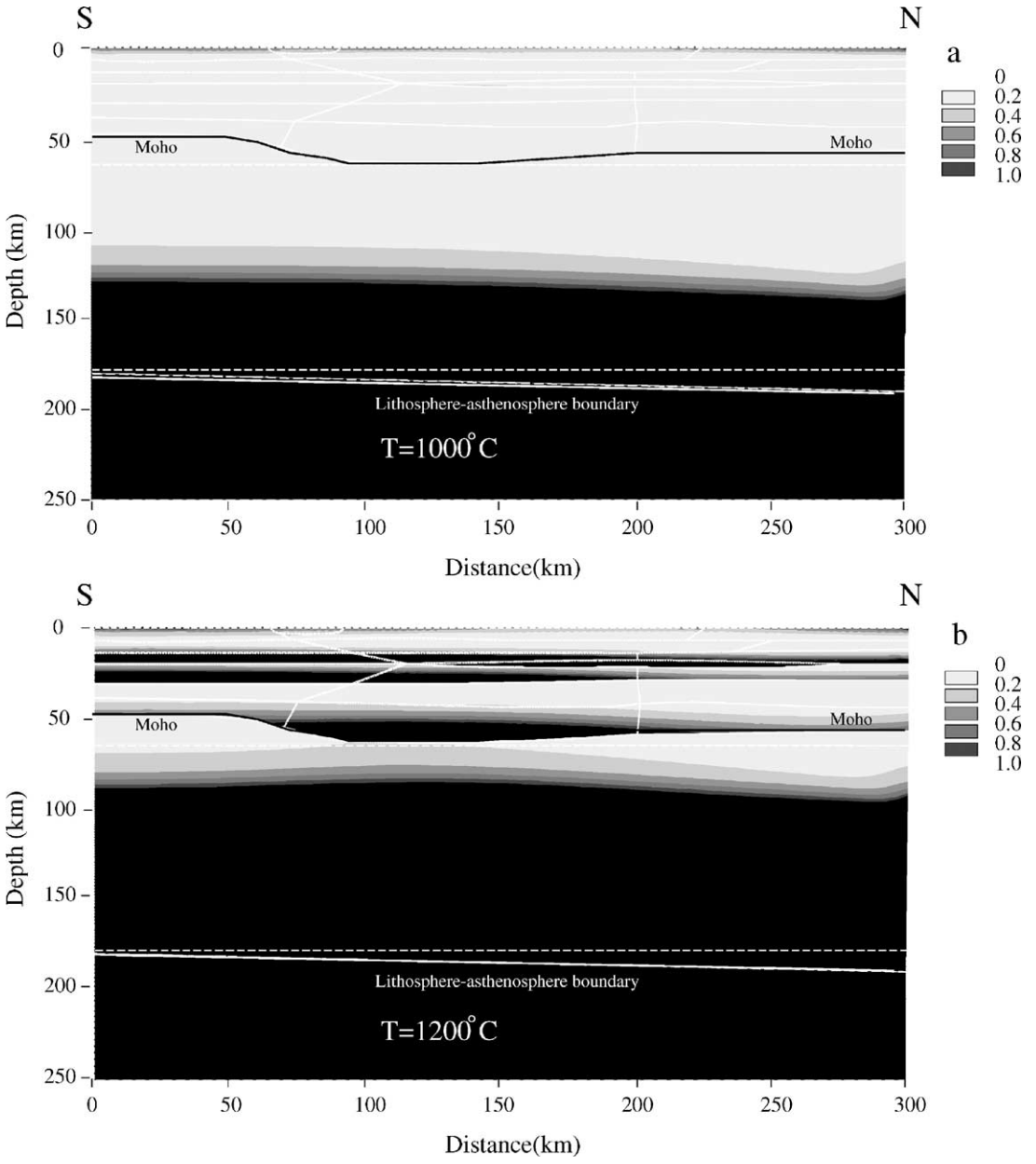

Fig. 13. The stress ratio for the structural model calculated (a) with the low temperature (T = 1000 °C) and (b) with high temperature variant (T = 1200 °C).

The stress ratio for the model calculated with the low temperature (T = 1000 °C, Fig. 13a) and the high temperature (T = 1200 °C, Fig. 13b) variants shows how the possible areas of deformation develop as a result of different temperature. Comparison with Fig. 9 shows the major differences. In the high temperature model zones of deformation in the crust are much thicker and also the depth where plastic deformation begins in the mantle is shifted upwards by 10–20 km. In the low temperature model no areas of deformation are found. In the thick lithosphere model (T = 1400 °C) stress ratio remains very similar as in the reference model.

Although the differences in the rheological strength due to temperature are rather large the effects in the stress intensity are much more balanced but still notable. The stress ratio, however, shows the overall result of the used rheological strength and the affecting stress field and a rather large difference between the different structural models can be observed. However, the thick lithosphere model (T = 1400 °C) has only minor effects on the rheology and the structural model, which is reasonable as the temperature difference in comparison with the reference model is quite moderate.

5. Conclusions

The two-dimensional rheological model for the FENNIA profile shows that in the central Fennoscandian Shield rheologically weak crustal layers can be generated under suitable conditions. A very important factor is an assumption of the wet crustal conditions for ductile creep properties. These layers are not only found in the lower crust but also in the upper and middle crust. For the dry conditions one weak layer is generated in the middle crust. In the mantle ductile strength is reduced to significantly low values at the depth of 110 km. Although such weak layers are found the application of the rheological structure to a model, where stress and deformation are derived does not yield a very significant crustal deformation. The crustal deformation is limited with both the wet and dry conditions to the very narrow zones in the upper and middle crust. In the mantle significant deformation begins at the depth of 100 km. In the stress fields distortions generated by the rheological structure are very small in the crust whereas in the mantle a very sharp boundary is generated. It is important to notice the uncertainties involved in these calculations in the form of temperature, strain rate, rheological parameters etc. We analysed more thoroughly the effects of temperature by using three thermal model variants with large uncertainty bounds (±100 °C at the depth of 50 km). This analysis shows that the effect of the temperature in the rheological and stress modellings is significant. However, these results give us an indication of what we should expect to occur in the deep lithosphere.

Acknowledgements

We wish to thank two anonymous reviewers for their useful comments and suggestions. Ansys is a trademark of Swanson Analysis System Inc.

References

Ahjos, T., Uski, M., 1992. Earthquakes in northern Europe in 1375–1989. Tectonophysics 207, 1–123.

Babuska, V., Plomerova, J., Padjusak, P., 1988. Seismologically determined deep lithosphere structure in Fennoscandia. Geologiska Föreningens i Stockholm Förhandlingar (GFF) 110, 380–382.

Blanpied, M.L., Lockner, D.A., Byerlee, J.D., 1991. Fault stability inferred from granite sliding experiments at hydrothermal conditions. Geophys. Res. Lett. 18, 609–612.

Calcagnile, G., 1982. The lithosphere-astonisher system in Fennoscandia. Tectonophysics 90, 19–35.

Carmichael, R.S., 1989. Practical Handbook of Physical Properties of Rocks and Minerals. CRC Press, Boca Raton, FL.

Carter, N.L., Tsenn, M.C., 1987. Flow properties of continental lithosphere. Tectonophysics 136, 27–63.

Chen, R., 1991. On horizontal crustal deformation in Finland, Rep. Finn. Geod. Inst., vol. 91:1. Helsinki, p. 77.

Cloetingh, S., Banda, E., 1992. Europe's lithosphere—physical properties. In: Blundell, D., Freeman, R., Mueller, St. (Eds.), A Continent Revealed: The European Geotraverse. Cambridge University Press, Cambridge, pp. 71–102.

Dragoni, M., Pasquale, V., Verdoya, M., Chiozzi, P., 1993. Rheological consequences of the lithospheric thermal structure in the Fennoscandian Shield. Global Plan. Change 8, 113–126.

FENNIA Working Group, 1998. P- and S-velocity Structure of the Fennoscandian Shield beneath the FENNIA Profile in Southern Finland. Report S-38. Institute of Seismology, University of Helsinki, p. 14.

Fernàndez, M., Ranalli, G., 1997. The role of rheology in extensional basin formation modelling. Tectonophysics 282, 129–145.

Gaal, G., Gorbatschev, R., 1987. An outline of the Precambrian evolution of Baltic Shield. Precambrian Res. 35, 15–52.

Goetze, C., Evans, B., 1979. Stress and temperature in the bending lithosphere as constrained by experimental rock mechanics. Geophys. J. R. Astr. Soc. 59, 463–478.

Haapala, I., Rämö, O.T., 1992. Tectonic setting and origin of the Proterozoic rapakivi granites of southeastern Fennoscandia. Trans. R. Soc. Edinb., Earth Sci. 83, 165–171.

Holbrook, W.S., Mooney, W.D., Christensen, N.I., 1992. The seismic velocity structure of the deep continental crust. In: Fountain, D.M., Arculus, R., Kay, R.W. (Eds.), Continental Lower Crust. Elsevier, Amsterdam, pp. 1–43.

Jokinen, J., Kukkonen, I., 1999. Random modelling of the lithospheric thermal regime: forward simulations applied in uncertainty analysis. Tectonophysics 306, 277–292.

Kaikkonen, P., Moisio, K., Heeremans, M., 2000. Thermomechanical lithospheric structure of the central Fennoscandian Shield. Phys. Earth Planet. Inter. 119, 209–235.

Kakkuri, J., 1997. Postglacial deformation of the Fennoscandian crust. In: Pesonen, L.J. (Ed.), The Lithosphere in Finland – a Geophysical Perspective. Geophysica, 33, pp. 99–109.

Klasson, H., Lejon, B., 1990. Rock Stress Measurements in the Deep Boreholes at Kuhmo, Hyrynsalmi, Sievi, Eurajoki and Konginkangas, Technical Report YJT-90-18. Nuclear Waste Commission of Finnish Power Companies, p. 122.

Koistinen, T., Klein, V., Koppelmaa, H., Korsman, K., Lahtinen, R., Nironen, M., Puura, V., Saltykova, T., Tikhomirov, S., Yanovskiy, A., 1996. Paleoproterozoic Svecofennian orogenic belt in the surroundings of the Gulf of Finland. In: Koistinen, T.J. (Editor), Explanation to the map of Precambrian basement of the Gulf of Finland and surrounding area 1:1 mill. Geol. Surv. Finland, Spec. Paper 21, pp. 21–57.

Korsman, K., Korja, T., Pajunen, M., Virransalo, P., 1999. The GGT/SVEKA transect. Structure and evolution of the continental crust in the Paleoproterozoic Svecofennian orogen in Finland. Int. Geol. Rev. 4, 287–333.

Kozlovskaya, E., Yliniemi, J., 1999. Deep structure of the Earth's crust along the SVEKA profile and its extension to the north-east. Geophysica 35, 111–123.

Kukkonen, I.T., 1988. Terrestrial heat flow and groundwater circulation in the bedrock in the central Baltic Shield. Tectonophysics 156, 59–74.

Kukkonen, I.T., 1989. Terrestrial Heat Flow in Finland, the Central Fennoscandian Shield, Report YST-68. Geological Survey of Finland, Nuclear Waste Disposal Research, p. 99.

Kukkonen, I.T., 1993. Heat flow map of northern and central parts of the Fennoscandian Shield based on geochemical surveys of heat producing elements. Tectonophysics 225, 3–13.

Kukkonen, I.T., 1998. Temperature and heat flow density in a thick cratonic lithosphere: The SVEKA transect, central Fennoscandian Shield. J. Geodyn. 26, 111–136.

Kukkonen, I.T., Lahtinen, R., 2001. Variation of radiogenic heat production rate in 2.8–1.8 Ga old rocks in the central Fennoscandian Shield. Phys. Earth Planet. Inter. 126, 279–294.

Kukkonen, I.T., Peltonen, P., 1999. Xenolith-controlled geotherm for the central Fennoscandian Shield: implications for lithophere–asthenosphere relations. Tectonophysics 304, 301–315.

Kukkonen, I.T., Kinnunen, K.A., Peltonen, P., 2003. Mantle xenoliths and thick lithosphere in the Fennoscandian Shield. Phys. Chem. Earth 28, 349–360.

Moisio, K., Kaikkonen, P., Beekman, F., 2000. Rheological structure and dynamical response of the DSS profile BALTIC in the SE Fennoscandian Shield. Tectonophysics 320, 175–194.

Moisio, K., Kaikkonen, P., 2001. Geodynamics and rheology along the DSS profile SVEKA'81 in the central Fennoscandian Shield. Tectonophysics 340, 61–77.

Nironen, M., 1997. The Svecofennian Orogen: a tectonic model. Precambrian Res. 86, 21–44.

Pasquale, V., Verdoya, M., Chiozzi, P., 2001. Heat flux and the seismicity in the Fennoscandian Shield. Phys. Earth Planet. Inter. 126, 147–162.

Ranalli, G., 1995. Rheology of the Earth, second ed. Chapman & Hall, London.

Rudnick, R.L., Fountain, D.M., 1995. Nature and composition of the continental crust: a lower crustal perspective. Rev. Geophys. 33, 267–309.

Sandoval, S., Kissling, E., Ansorge, J., SVEKALAPKO Seismic Tomography Working Group, 2004. High-resolution body wave tomography beneath the SVEKALAPKO array—II. Anomalous upper mantle structure beneath the central Baltic Shield. Geophys. J. Int. 157, 200–214.

Saari, J., 1992. A Review of the Seismotectonics of Finland, Report YJT-92-99. Nuclear Waste Commission of Finnish Power Companies, p. 76.

Scholz, C.H., 1990. The Mechanics of Earthquakes and Faulting. Cambridge University Press, Cambridge.

Wilks, J.C., Carter, N.L., 1990. Rheology of some continental lower crustal rocks. Tectonophysics 182, 57–77.

Windley, B., 1992. Precambrian Europe. In: Blundell, D., Freeman, R., Mueller, St. (Eds.), A Continent Revealed: The European Geotraverse. Cambridge University Press, Cambridge, pp. 139–214.